Design A Robust Power System Stabilizer on SMIB Using Lyapunov Theory

Yin Li, *Student Member, IEEE*, Lingling Fan, *Senior Member, IEEE*

***Abstract*—This paper proposes a robust power system stabilizer (PSS) using Lyapunov Stability theory introduced in Optimization & Control in Power System class at University of South Florida. This research examines the robustness of the novel PSS in the synchronous generator connected to an infinite bus (SMIB) system under multiple operation conditions. After deriving the state space matrices of the linear model of the system, the gains of robust PSS are estimated using Lyapunov function in the linear matrix inequality (LMI). The model analyzed in this paper is an electromagnetic model with automatic voltage regulator (EMT+AVR). Then, EMT+AVR model with the robust PSS is analyzed and compared with the conventional PSS. In the simulation part, the nonlinear simulation is conducted in MATLAB/Simulink to compare the conventional PSS and novel PSS.**

***Index Terms*—SMIB, EMT+AVR, PSS, Lyapunov theory, LMI.**

I. Introduction

Power system stabilizer (PSS) is used to introduce an auxiliary signal to automatic voltage regulator (AVR). When power output from a generator is at high level, electromechanical oscillation will be dominant with a fast exciter and large gain of the amplifier in AVR which make the poles move to right half plane (RHP) easily [1]. The function of conventional PSS is to change the root locus to avoid poles moving to RHP by adding one pole and two zeros of the system transfer function. However, its design is based on a linearized model of a certain operating condition. It may not work well when the operating condition changes.

The objective of this paper is to design a PSS that can work for a range of operating conditions, so the novel PSS or robust PSS has much better robustness. In addition, the selected values for robust PSS gains can be estimated using CVX toolbox of MATLAB rather than manually selecting like conventional PSS. Different than conventional PSS, robust PSS only contains a state feedback gain matrix, K, which has the same size as the system outputs. It is assumed that K is existing using linear-quadratic regulator (LQR). Then, Lyapunov stability theory which is introduced in Optimization & Control in Power System class is used to write a Lyapunov function with K in (LMI). Finally, the existing K can be estimated using CVX toolbox when each of linear matrix inequality constraint which is corresponding to each operating condition is satisfied.

Before design robust PSS, the EMT+AVR model of SMIB system will be linearized in state space in Section II. Section III does not only introduce the design of robust PSS, but also compare it with conventional PSS under several operating conditions. The linear analysis results will be also validated by nonlinear simulations which are tested in MATLAB/Simulink in simulation part.

Y. Li and L. Fan are with Dept. of Electrical Engineering, University of South Florida, Tampa FL 33620. Email: linglingfan@usf.edu.

II. Linear Plant Model

Synchronous generator connected to an infinite bus shown in Fig. 1 is the typical power system in Chapter 7 of a classic textbook "Power System Analysis" [1] used in EEL 6936 Power Systems II at University of South Florida. It is normally used to analyze the effect of AVR and PSS on the power system. The rotor of the synchronous generator is salient-pole and its damper is assumed to be ignored, so $i_D = i_Q = 0$. Except stator resistance, r_s, all of resistances and inductances of the rotor and stator are considered, r_f, L_f, L_d, and L_q. The scripts, $_d$ and $_q$, mean the components in dq frame. X is the impedance of the corresponding inductance. Certainly, the transmission line impedance, X_L, is included for linear analysis.

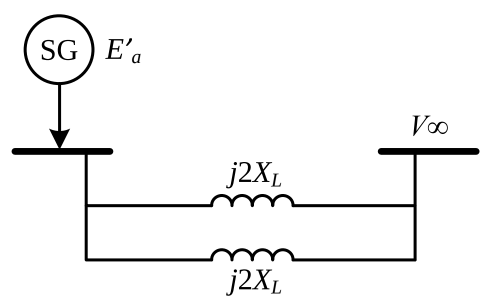

Fig. 1. A generator connected to an infinite bus.

A. EMT+AVR model

According to the linear model of SMIB system derived in [1] using steady state analysis, the EMT+AVR model in this paper has four state variables, $\Delta\delta$, $\Delta\omega$, $\Delta E'_a$, and E_{fd}, because the dynamics of the exciter is considered, T_e. Therefore, Fig. 2 presents the block diagram of the linear EMT+AVR model.

H and D are the inertial and damping of the synchronous generator while the gains from k_1 to k_6 (k_1=T) are calculated if the initial real power and reactive power, P_m and Q, are provided. P_m and Q can determine the transient stator voltage, $|E'_a|$, and the phase angle of the stator voltage, δ, using (1).

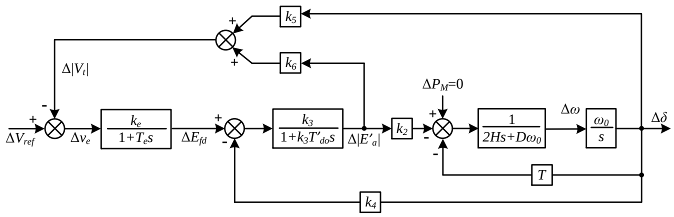

Fig. 2. Block diagram of EMT+AVR model.

$$
\begin{aligned}
P_m = P_e &= \frac{|E'_a||V_\infty|}{\widetilde{X'_d}}\sin(\delta) + \frac{|V_\infty|^2}{2}\left(\frac{1}{\widetilde{X_q}} - \frac{1}{\widetilde{X'_d}}\right)\sin(2\delta) \\
Q &= \frac{|E'_a||V_\infty|}{\widetilde{X'_d}}\cos(\delta) - |V_\infty|^2\left(\frac{\cos^2(\delta)}{\widetilde{X'_d}} + \frac{\sin^2(\delta)}{\widetilde{X_q}}\right)
\end{aligned}
\tag{1}
$$

Then, using (2) from [2] to calculate the initial values of k_1 to k_6 to build linear model after obtaining $|E'_a|$ and δ.

$$
\begin{aligned}
k_1 &= \frac{|E'_a||V_\infty|}{\widetilde{X'_d}}\cos(\delta) + |V_\infty|^2\left(\frac{1}{\widetilde{X_q}} - \frac{1}{\widetilde{X'_d}}\right)\cos(2\delta) \\
k_2 &= \frac{V_\infty}{\widetilde{X'_d}}\sin(\delta) \\
k_3 &= \frac{\widetilde{X'_d}}{\widetilde{X_d}} \\
k_4 &= \frac{\widetilde{X_d}}{\widetilde{X'_d} - 1} \\
k_5 &= -|V_\infty|\left(\frac{X'_d V_{aq}}{\widetilde{X'_d}|V_a|}\sin(\delta) + \frac{X_q V_{ad}}{\widetilde{X_q}|V_a|}\cos(\delta)\right) \\
k_6 &= \frac{X_L V_{aq}}{\widetilde{X'_d}|V_a|}
\end{aligned}
\tag{2}
$$

B. State Space

Because Lyapunov function is the function of the state space, the state space matrices of EMT+AVR model, A, B, C, and D, should be derived. According to its block diagram shown in Fig. 2, A and B matrices can be found easily if ΔV_{ref} is considered as the input.

$$
\frac{d}{dt}\begin{bmatrix}\Delta\delta \\ \Delta\omega \\ \Delta E'_a \\ \Delta E_{fd}\end{bmatrix} = \underbrace{\begin{bmatrix} 0 & \omega_0 & 0 & 0 \\ -\frac{T}{2H} & -\frac{D\omega_0}{2H} & -\frac{k_2}{2H} & 0 \\ -\frac{k_4}{T'_{do}} & 0 & -\frac{1}{k_3 T'_{do}} & \frac{1}{T'_{do}} \\ -\frac{k_5 k_A}{T_e} & 0 & -\frac{k_6 k_A}{T_e} & -\frac{1}{T_e}\end{bmatrix}}_{A}\begin{bmatrix}\Delta\delta \\ \Delta\omega \\ \Delta E'_a \\ \Delta E_{fd}\end{bmatrix} + \underbrace{\begin{bmatrix}0 \\ 0 \\ 0 \\ \frac{k_A}{T_e}\end{bmatrix}}_{B} U
\tag{3}
$$

Normally, the feedback of input on the output is neglected, $D = 0$. Due to the limitation of Lyapunov function which will be mentioned in next section, C matrix has to be a unit matrix. Hence, four state variables are also the outputs.

$$
Y = \underbrace{\begin{bmatrix}1 & 0 & 0 & 0 \\ 0 & 1 & 0 & 0 \\ 0 & 0 & 1 & 0 \\ 0 & 0 & 0 & 1\end{bmatrix}}_{C}\begin{bmatrix}\Delta\delta \\ \Delta\omega \\ \Delta E'_a \\ \Delta E_{fd}\end{bmatrix}
\tag{4}
$$

III. Robust PSS Using Lyapunov Theory

Although AVR makes the SMIB system transfer more power, the power transfer level (δ) of EMT+AVR model is relative low, so the system will become unstable even if δ is still small [2]. Power system stabilizer (PSS) is the general method to increase the power transfer level.

A. Conventional PSS

The conventional PSS makes the EMT+AVR model stable by changing the root locus of the system. There are one pole and two zeros added shown in Fig. 3.

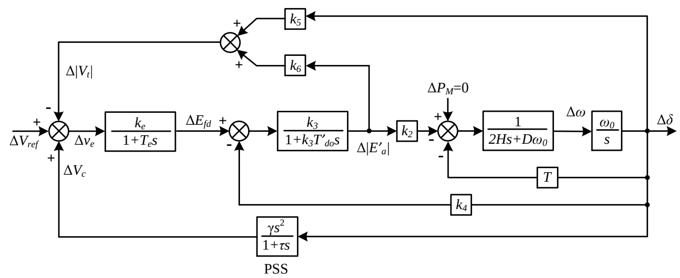

Fig. 3. The block diagram of EMT+AVR model with conventional PSS.

The parameters of conventional PSS, τ and γ, are designed by manually tuning, so the selected values of τ and γ cannot make sure that the system is always stable under a lot of conditions like power changing or faults occurring. Therefore, the robustness of conventional PSS is limited.

For example, in this paper, there are twenty-five different combinations of real power and reactive power, P_m and Q, generated by the synchronous machine. In addition, the fault on the transmission line is considered, so its impedance will be double after the fault based on Fig. 1. Hence, the total number of conditions is fifty and listed in Table I.

The system stability can be used to verify the effect of PSS on EMT+AVR model. For linear analysis, the eigenvalues of A matrix is one kind of method to determine the system stability. Ten conditions listed in Table I are selected randomly to test the system stability including EMT+AVR model and EMT+AVR+PSS model. The elements in the corresponding A matrices are calculated using P_m and Q listed in Table I and the system parameters listed in Table V. The eigenvalues of corresponding A matrices are found using MATLAB code and listed in Table II. It is observed that each of A matrices for Cond1 and Cond7 has two eigenvalues including positive real parts. It means that the system is unstable under Cond1 and Cond7.

To find the effect of conventional PSS on EMT+AVR model, the four dominant eigenvalues of EMT+AVR model integrated

TABLE I
50 CONDITIONS.

$X_L = 0.4$					
P(p.u.) \ Q(p.u.)	-0.8	-0.5	0	0.5	0.8
1.28	Cond1	Cond2	Cond3	Cond4	Cond5
1.26	Cond6	Cond7	Cond8	Cond9	Cond10
1.0	Cond11	Cond12	Cond13	Cond14	Cond15
0.8	Cond16	Cond17	Cond18	Cond19	Cond20
0.6	Cond21	Cond22	Cond23	Cond24	Cond25
$X_L = 0.2$					
P(p.u.) \ Q(p.u.)	-0.8	-0.5	0	0.5	0.8
1.28	Cond26	Cond27	Cond28	Cond29	Cond30
1.26	Cond31	Cond32	Cond33	Cond34	Cond35
1.0	Cond36	Cond37	Cond38	Cond39	Cond40
0.8	Cond41	Cond42	Cond43	Cond44	Cond45
0.6	Cond46	Cond47	Cond48	Cond49	Cond50

TABLE II
EMT+AVR: EIGENVALUES OF A UNDER DIFFERENT CONDITIONS.

	Eig 1, 2	Eig 3,4
Cond1	-2.3626 ± 5.2994i	1.0977 ± 4.7385i
Cond7	-1.3975 ± 5.6237i	0.1326 ± 5.1232i
Cond15	-1.1084 ± 4.5614i	-0.1565 ± 8.3052i
Cond17	-0.8392 ± 5.9651i	-0.4257 ± 4.1992i
Cond22	-0.7872 ± 6.0819i	-0.4777 ± 3.7036i
Cond28	-0.9304 ± 3.8556i	-0.5012 ± 8.9879i
Cond34	-1.1593 ± 3.8652i	-0.2723 ± 9.4164i
Cond39	-1.1213 ± 3.9069i	-0.3102 ± 9.7459i
Cond43	-0.9701 ± 3.6145i	-0.4614 ± 8.2878i
Cond50	-1.3050 ± 3.9187i	-0.1266 ± 9.4927i

by conventional PSS are found and listed in Table III. 0.001 and 0.1 are selected for γ and τ. Although the system becomes stable under Cond7 by adding conventional PSS, the limited robustness of conventional PSS cannot make the system stable under Cond1.

TABLE III
EMT+AVR+CONVENTIONAL PSS: EIGENVALUES OF A UNDER DIFFERENT CONDITIONS.

	Eig 1, 2	Eig 3,4
Cond1	-2.1795 ± 5.3098i	0.9911 ± 4.7780i
Cond7	-0.8991 ± 5.7661i	-0.2979 ± 5.0637i
Cond15	-1.0997 ± 4.5137i	-0.1345 ± 8.3666i
Cond17	-0.7150 ± 6.1821i	-0.4814 ± 4.0291i
Cond22	-0.6996 ± 6.2538i	-0.4990 ± 3.5808i
Cond28	-0.9206 ± 3.7816i	-0.4377 ± 9.0965i
Cond34	-1.1459 ± 3.8165i	-0.2342 ± 9.4882i
Cond39	-1.1092 ± 3.8548i	–0.2659 ± 9.8220i
Cond43	-0.9550 ± 3.5458i	-0.4097 ± 8.3936i
Cond50	-1.2950 ± 3.8908i	-0.1072 ± 9.5335i

B. Robust PSS Design

The novel PSS using Lyapunov theory has a much better robustness because its gains are estimated by MATLAB CVX toolbox rather than manually tuning. The novel robust PSS does not have poles or zeros, but the pure gain matrix, K. If the state space of a specific system is known (5),

$$\begin{cases} \dot{x} = Ax + Bu \\ y = Cx \end{cases} \tag{5}$$

A state feedback gain matrix, K, is designed to generate output static feedback to replace the input using LQR (6).

$$u = Ky = KCx \tag{6}$$

Substituting (6) into $\dot{x}$ function of (5),

$$\dot{x} = Ax + BKCx = (A + BKC)x \tag{7}$$

It is easily to find that A matrix becomes $A+BKC$, so the system will be stable if a existing K is found to make the real parts of eigenvalues of $(A + BKC)$ negative. In this paper, K is a 1X4 matrix because of (3) and (4). Therefore, each of output or state variable has a corresponding gain to generate the static feedback shown in Fig. 4. The sum of feedback is named as the compensated voltage, ΔV_c, and is added to the input.

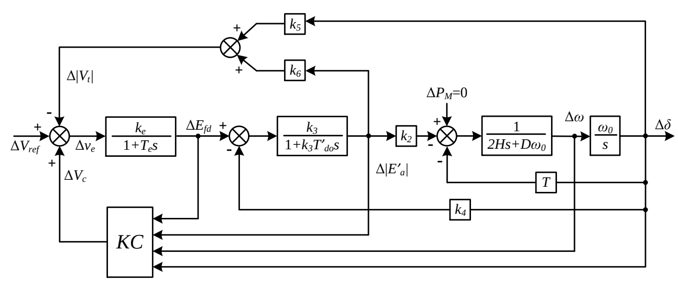

Fig. 4. The block diagram of EMT+AVR model with robust PSS.

To find K, the Lyapunov function needs to be expressed in LMI.

$$\begin{aligned} 0 \geq& (A + BKC)^T P + P(A + BKC) + \beta P \\ 0 \geq& (A + BKC)^T + P(A + BKC)P^{-1} + \beta \\ 0 \geq& A^T + C^T K^T B^T + PAP^{-1} + PKCP^{-1} + P \\ 0 \geq& P^{-1}A^T + P^{-1}C^T K^T B^T + AP^{-1} + BKCP^{-1} + P^{-1}\beta \end{aligned} \tag{8}$$

where P is semi-definite and has the same size as A matrix; β is a constant which is greater than zero. If $X = P^{-1}$ and $Y = KCP^{-1}$, (8) will be rewritten as:

$$\begin{aligned} 0 \geq XA^T + Y^T B^T + AX + BY + X\beta \\ X \geq 0 \end{aligned} \tag{9}$$

CVX toolbox of MATLAB is employed to find the existing X and Y to satisfy LMI constrain. Each of LMI constrain is corresponding to each operating condition. After X and Y are found, the gain matrix of robust PSS can be can calculated using $K = YX^{-1}C^{-1}$. If the robustness of PSS needs to be increased, multiple conditions of the system should be considered because one gain matrix, K, found by CVX can satisfy all of LMI constrains. It means that more conditions considered causes the better robustness of PSS. The following code is using CVX toolbox to find K.

```
cvx_begin sdp
variable X(n,n) symmetric
variable Y(1,n)
X*A1'+ Y'*B'+A1*X+B*Y+X*beta <=0
X*A2'+ Y'*B'+A2*X+B*Y+X*beta <=0
              .
              .
              .
X>=eye(n)
cvx_end
KC=Y*inv(X)
```

where n presents the size of A matrix. In Lyapunov function, P matrix must be symmetric, so the constrain of symmetric should be added to X matrix. Based on (3) and (4), only A matrix is changed corresponding to different conditions because the exciter of the system is normally not variable. Each condition has one specific set of initial values to generate a specific A matrix using (2), so how many A matrices is equal to how many considered conditions. Due to C is the unit matrix (4), $K = KC = YX^{-1}$.

After running CVX code, the state feedback gain matrix is estimated:

```
KC =
   1.0e+03 *

    0.0080    7.6136   -0.1016   -0.0004
```

After applying the robust PSS to EMT+AVR model, the eigenvalues of new A matrices, $A+BKC$, are calculated and listed in Table IV. Compared with the eigenvalues listed in Table **??**, the real parts of all eigenvalues in Table IV are negative besides eigenvalues of Cond1 and Cond7. Therefore, it is concluded that the robust PSS has the better robustness on the stability of EMT+AVR model.

TABLE IV
EMT+AVR+ROBUST PSS: EIGENVALUES OF $(A + BKC)$ UNDER DIFFERENT CONDITIONS.

	Eig 1, 2	Eig 3,4
Cond1	-4.2411 &-9.3056	-8.7674 ±53.0810i
Cond7	-6.5566 ± 2.6118i	-8.9842 ±53.0798i
Cond15	-3.4965 ± 7.9962i	-12.0443 ±53.1654i
Cond17	-6.2844 ± 2.6568i	-9.2564 ±53.0578i
Cond22	-5.9135 ± 2.8572i	-9.6273 ±53.0474i
Cond28	-8.6645 ± 4.6601i	-7.0430 ±53.3120i
Cond31	-6.2087 ± 7.9191i	-9.4988 ±53.0371i
Cond39	-7.1413 ± 7.6704i	-8.5662 ±53.0953i
Cond43	-7.1527 ± 5.3502i	-8.5547 ±53.1131i
Cond50	-3.4588 ± 9.2725i	-12.2486 ±53.1455i

IV. SIMULATION RESULTS FROM NON-LINEAR MODEL

The nonlinear EMT+AVR models with conventional PSS and robust PSS are designed and simulated in MATLAB/Simulink using the differential equations from [1], [2]. The selected γ and τ and the estimated K are applied to the corresponding non-linear models to verify the robustness of two PSS. Fig. 5 presents the screen shot of the non-linear EMT+AVR+PSS model.

The techniques for building non-linear model are detailed presented in [3] and are also applied in variety of system [4], [5]. For example, the vector feature technique is employed. Three of four state variables, E_a', δ, and ω, are arranged in a vector and generated by integrating their derivatives from Embedded MATLAB Function which contains the differential equations.

The initial values for four state variables should be calculated to make the flat run before the step change. When the flat run, the output of the exciter, $\frac{k_A}{T_e s+1}$, is zero, so the initial value of E_{fd} is not required. The synchronous generator is assumed at the rated speed, so the initial value of ω is $1p.u.$ Therefore, only the initial values of E_a' and δ requires to be calculated based on P_m and Q from conditions and system parameters listed in Table V.

TABLE V
PARAMETERS OF THE SYSTEM.

Parameter	Value(p.u.)
$V_{\inf}$	1
Speed, ω	1
H	5
D	0.003
T_e	0.8s
K_A	50
X_d, X_q	1, 0.7
r_f, X_{fd}	0.05, 0.1
X_L, X_d'	0.2, 0.2

A. Conventional PSS

Compared with linear analysis, the system stability of a non-linear model can be determined by the step response, so there was a step change, $0.01p.u.$, added to the input, V_{ref}. Corresponding to the unstable conditions analyzed in Section III, Cond1 and Cond7 were selected to calculate the initial values; then, start to run the non-linear models with the flat run. The step change happened at 10s, so the step responses of five measurements in EMT+AVR+conventional PSS model under Cond1 and Cond7 appeared after 10s shown in Fig. 6 and Fig. 7. The five measurements are terminal voltage, V_t, compensator voltage from PSS, V_c, stator voltage angle, δ, generator frequency, ω, and generated real power, P_e

Fig. 7 showed that the system became stable after several seconds while Fig. 6 presented a unstable system because the step responses became larger and larger rather than approaching a constant. It verified that the conventional PSS cannot make the system stable under both of operation conditions. Moreover, one cycle of the oscillation wave in Fig. 7 was around 1.2s, so the oscillation frequency, ω_{osc}, was $5.24rad/s$. The non-linear model was verified to have the same dynamics of its corresponding linear model because the imaginary part of eigenvalues of Cond7 in Table III was the same as ω_{osc}.

B. Robust PSS

In the linear analysis section, the system is always stable after applying robust PSS to EMT+AVR model, even if it is under Cond1. The simulation results of non-linear

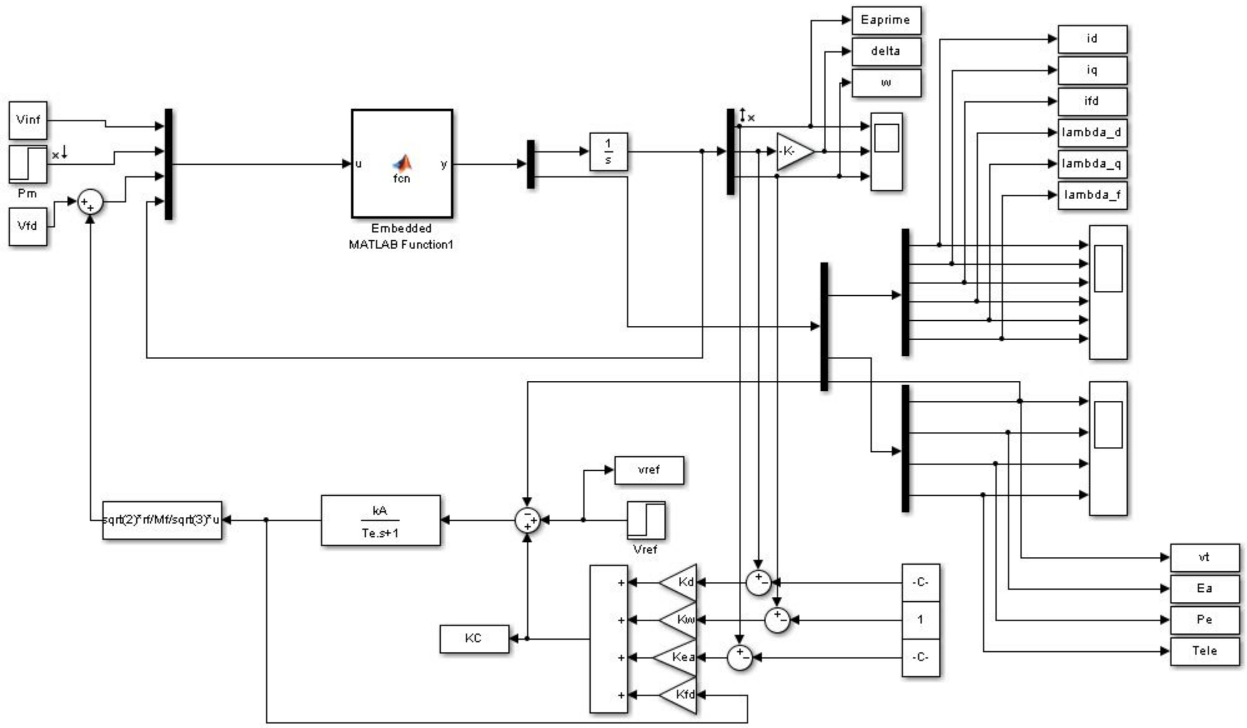

Fig. 5. The non-linear EMT+AVR+PSS model based on SMIB systems is designed in MATLAB

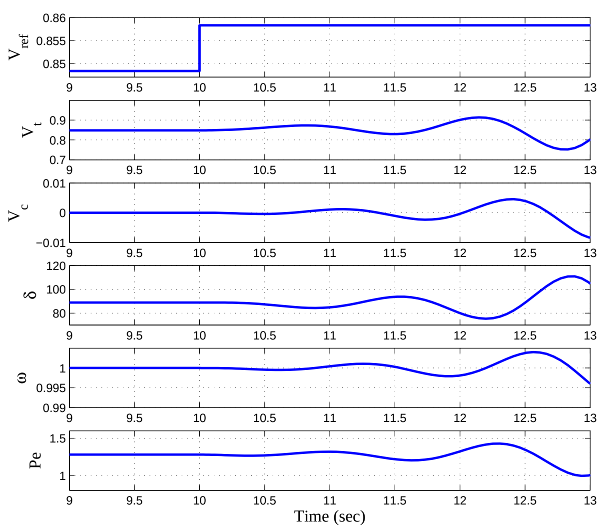

Fig. 6. The step responses of SMIB system with conventional PSS under Cond1.

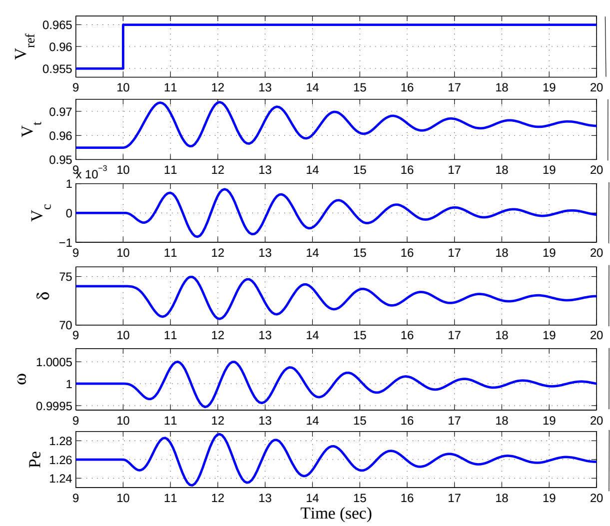

Fig. 7. The step responses of SMIB system with conventional PSS under Cond7.

EMT+AVR+robust PSS model verified this point. The simulation results were plotted in Fig. 8 and Fig. 9. It was observed that all of step responses were stable after the step change regardless of Cond1 and Cond7. Furthermore, robust PSS has the faster response speed and smaller oscillation. It can be proved by Table III and Table IV because the eigenvalues in Table IV have larger damping and are further away from the imaginary axis.

V. Conclusion

A novel robust power system stabilizer (PSS) is proposed in this paper and its effect on the stability of SMIB system is analyzed. Compared with the conventional PSS, the parameter or gain matrix of the robust PSS are estimated by CVX code rather than selected manually. Because the gain matrix can be estimated based on multiple operating conditions, this kind of PSS has the much better robustness. CVX toolbox is a good tool to find the state feedback gain matrix of Lyapunov

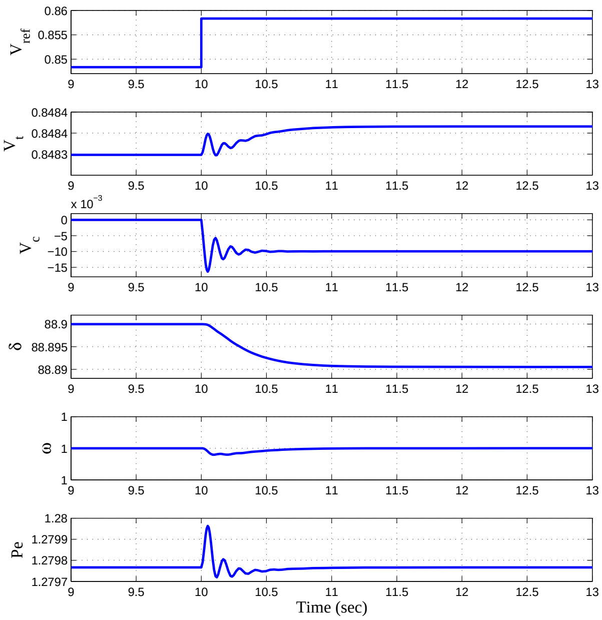

Fig. 8. The step responses of SMIB system with robust PSS under Cond1.

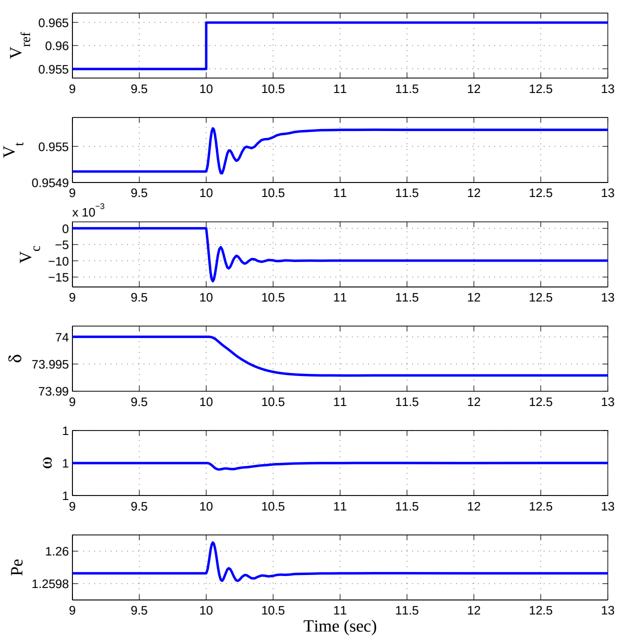

Fig. 9. the step responses of SMIB system with robust PSS under Cond7.

function expressed in LMI. Certainly, the SMIB system should be linearized to derive its state space matrices before the estimation. By comparing the eigenvalues, the effect of robust PSS on the linear EMT+AVR is presented. The simulation results from the corresponding non-linear models gave a strong support to the results from the linear analysis. Although this robust PPS is only applied to a simple power system in this paper, it has a huge potential on the complex and variable power systems due to its good robustness.

REFERENCES

[1] A. Bergen and V. Vittal, "Power systems analysis (second edition)," 1999.

[2] Y. Li and L. Fan, "Determine power transfer limits of an smib system through linear system analysis with nonlinear simulation validation," in *North American Power Symposium (NAPS), 2015*, Oct 2015, pp. 1–6.

[3] Z. Miao and L. Fan, "The art of modeling and simulation of induction generator in wind generation applications using high-order model," *Simulation Modelling Practice and Theory*, vol. 16, no. 9, pp. 1239–1253, 2008.

[4] L. Fan, R. Kavasseri, Z. L. Miao, and C. Zhu, "Modeling of dfig-based wind farms for ssr analysis," *Power Delivery, IEEE Transactions on*, vol. 25, no. 4, pp. 2073–2082, 2010.

[5] L. Fan, Z. Miao, S. Yuvarajan, and R. Kavasseri, "Hybrid modeling of dfigs for wind energy conversion systems," *Simulation Modelling Practice and Theory*, vol. 18, no. 7, pp. 1032–1045, 2010.